

# Effect of temperature on the transmission loss of large-core optical fiber

ALHADI ALARABI<sup>a,b</sup>, JINZHONG WANG<sup>a,\*</sup>, HONG-HU MA<sup>a</sup>, DONGBO WANG<sup>a</sup>, QINGJIANG YU<sup>a</sup>, SHIYONG GAO<sup>a</sup>, SHUIE JIAO<sup>a</sup>, YONG ZHANG<sup>a</sup>, JAMES TABAN<sup>a</sup>, AMANY ABDELLAH<sup>a</sup>, XIA ZHAO<sup>c</sup>, LIHUA LIU<sup>c</sup>

<sup>a</sup>Department of Optoelectronic Information Science, School of Materials Science and Engineering, Harbin Institute of Technology, Harbin 150001- China

<sup>b</sup>Department of Physics, University of Kassala, P. O. Box 266; Kassala, Sudan

<sup>c</sup>Fasten Company, Jiangyin, Jiangsu 214433, China

In this study, a large-core optical fiber is fabricated by modified chemical vapor deposition (MCVD) was employed and the effects of temperature on its optical properties were investigated. At a temperature range of  $-100^{\circ}\text{C}\sim 100^{\circ}\text{C}$ , it was found that the transmission loss coefficient of the first window (850 nm band) was changed at a range of 2.487dB/km  $\sim$  4.27dB/km, and at the range of 0.96dB/km  $\sim$  7.575dB/km for the second window (1050 nm band). Further the transmission loss is increased at the end of both high and low-temperature sides and a large fluctuation was notices. Electron paramagnetic resonance indicated that there are no paramagnetic defects in the fiber. Additionally, it was also found that the optical transmission loss coefficient decreases gradually from 3.095dB/Km to 2.353dB/Km after 30 days then becomes stable.

(Received November 3, 2017; accepted June 7, 2018)

*Keyword:* Large-core optical fiber, MCVD, Effect of temperature, Transmission loss

## 1. Introduction

As a result of the fast development in optical fiber communication, the transmission of data by the method for optical strands is becoming more and more extensive application. A fiber-optics correspondence connect in a shuttle is one potential application, so it is critical to concentrate on the effect of the space environment on the strands. Under the extreme bad conditions, such as on a rocket those filaments might be subjected to a temperature extend as wide as  $120^{\circ}\text{C}$  to  $-150^{\circ}\text{C}$ . Both the high and low-temperature extremes may have critical effects on the preform of the fiber. File and stage changes in polymers utilized for cladding and solidifying and embrittlement of defensive coats can both result in undesirable constriction and troubles in keeping up adaptability of a fiber link [1].

The particular structure in the optical fiber is formed during the fabrication. Thus, it doesn't require extra post processing for manufacturing fiber sensing head. Enbang Li [2] shows a multimode fiber interference temperature sensor [2], and a temperature sensor operational up to  $800^{\circ}\text{C}$  employing the interference of several higher order Linearly Polarized (LP) methods in a multimode fiber-single-mode fiber-cleaved facet configuration. Jian Ju studied two-mode photonic crystal fiber and their sensitivity to temperature [3]. D. S. Moon researched a temperature sensor on the basis of the Sagnac interferometer made of polarization-maintaining fiber [4]. Fufei Pang et al. found that the temperature response was -

$20^{\circ}\text{C}$  to  $80^{\circ}\text{C}$  under the coating the optical fiber with temperature-sensitive silicone [5]. The result demonstrated good repeatability and high-temperature sensitivity. Also, the temperature increase due to the transmission power increase [5].

Xinghu Fu et al. [6] their experimental results showed that the sensitivities of  $72.17\text{ pm}^{\circ}\text{C}$  at range from  $35^{\circ}\text{C}\sim 95^{\circ}\text{C}$  with characteristics of insensitive to external refractive index in the range 1.3450 to 1.4607. Their result also that the sensor used for solution temperature controlling in real time. In most cases, glass optical fibers with low-temperature coatings are played an important role, and the measurements are restricted to relatively low temperatures [7]. Mehta et al. studied a displacement sensor created with a single-mode fiber-multimode fiber-mirror configuration [8]. Zhang and Peng [9] demonstrated a transmissive refractive index sensor using a Single mode-Multimode-Single mode structure (SMS). The transmission loss characteristics of multimode fiber spliced between Single mode-Multimode-Single mode (SMS devices) has been investigated by A Kumar et al. [10]. The SMS sensor using photonic crystal fiber was demonstrated to be capable of measuring  $500^{\circ}\text{C}$  [11]. Demas et al. demonstrated a fiber-optic sensor able of measuring up to  $1000^{\circ}\text{C}$  with a device taking advantage of a photonic crystal fiber (PCF) and a  $\text{CO}_2$  laser-written long-period grating [12-14]. Honda et al. investigated the temperature up to  $1000^{\circ}\text{C}$ , and they found the peaks from OH were spotted in the fibers and the intensity depends on

the temperature. They also state that when the temperature of F-doped fibers was kept at 1000°C, unexpected peaks showed and grew [15].

Until now, there were a few researches on large energy fiber at high and low temperature. In this study, time was described, EPR spectra, and temperature dependence of transmission loss. In addition, the high and low-temperature were demonstrated and the effects of temperature were studied. The optical fiber with fluorine content was prepared by modified chemical vapor deposition (MCVD).

## 2. Experiment

The optical fiber was fabricated by the MCVD method. The fiber consists of pure silica glass ( $SiO_2$ ) core with a diameter of 200  $\mu\text{m}$ , and a 220  $\mu\text{m}$  fluorine cladding doped outer diameter. In the MCVD fiber cladding, fluorine was used as dopants. EPR (X-band A200, German) was used in this study to show the defects in a sample. The details of the material and specifications and the parameters, as well as the composition of the optical fibers, are shown in Table 1.

Table 1. Materials and specifications of the perform optical fiber

Item	Unit	Indicators
Operating Wavelength	nm	800~1600
Numerical aperture (NA)		0.22±0.02
OH Level		Low
Coating Diameter	$\mu\text{m}$	320±15
Cladding Diameter	$\mu\text{m}$	220±3
Core Diameter	$\mu\text{m}$	200±4
Core/Clad Offset	$\mu\text{m}$	<5
Coating Material		Dual Acrylate
Working temperature	°C	-55°C~85°C

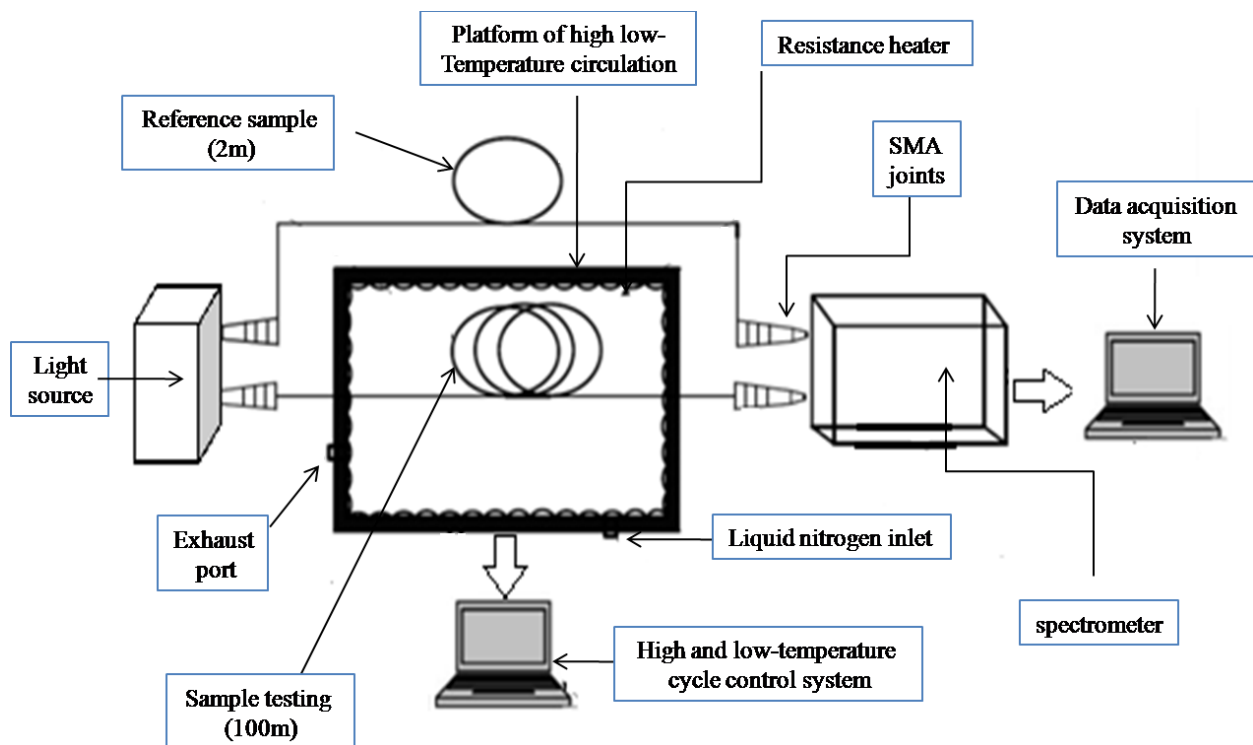


Fig. 1. Schematic diagram of high-low temperature cycle test of large-core energy optical fiber

### 2.1. High and low-temperature test

In the heat treatment, the temperature tests were done in Harbin Institute of Technology, Space Materials, and

Environment Engineering National Key Laboratory Spatial temperature. Fig. 1 shows the overview of this experiment, includes five-part: light source (380 nm-2500 nm), high and low-temperature cycle control system, data

acquisition system, an experimental platform of high-low temperature circulation and the spectrometer. One end of the optical fiber was connected to the light source, and the other end of the optical fiber was connected to an optical spectrometer analyzer (model AvaSpec-ULS2048 XL).

### 2.2. High and low-temperature test setup and data acquisition

Heating temperatures have been selected in the range ( $-100^{\circ}\text{C}$  to  $100^{\circ}\text{C}$ ). The cycling path was  $25^{\circ}\text{C} \rightarrow 100^{\circ}\text{C} \rightarrow 0^{\circ}\text{C} \rightarrow -100^{\circ}\text{C} \rightarrow 0^{\circ}\text{C} \rightarrow 25^{\circ}\text{C}$ . The typical diameter of the length of the sample fiber was 100m. Through experience, modifying the equipment of heating power, high low temperature using liquid of nitrogen to control flow speed, and increase the temperature of the device. To keep up the increasing temperature the cooling rate was  $0.9^{\circ}\text{C}/\text{min}$ , for every  $5^{\circ}\text{C}$  and the insulation was 10min. In order to get a uniform maximum temperature on the optical fiber in the experiment, aluminum foil was used to cover the optical fiber. For data collection, AvaSpec-ULS2048 XL-USB fiber optic spectrometer was used every  $5^{\circ}\text{C}$ . At room temperature ( $25^{\circ}\text{C}$ ), the length was 2m of the optical fiber was used as a reference value for transmission.

Signal attenuation in optical fibers was obtained in the logarithmic unit of the decibel. The decibel used for contrasting two power levels, and defined for a particular optical wavelength as the ratio of the output optical power ‘Po’ from the fiber to the input optical power ‘Pi’[16]. The equations below show how to calculate the attenuation losses:

$$\text{loss (dB)} = A(\lambda) = 10\log\left(\frac{P_{in}(\lambda)}{P_{out}(\lambda)}\right) \quad (1)$$

And the attenuation coefficient obtained by

$$\alpha(\lambda) = \frac{A(\lambda)}{L} = \frac{10\log\left[\frac{P_{in}(\lambda)}{P_{out}(\lambda)}\right]}{L} \quad (2)$$

So when we used temperature the attenuation coefficient expressed as:

$$\alpha(\lambda) = \frac{A(\lambda)}{L} = \frac{10\log\left[\frac{T_{ref}(\lambda)}{T_{out}(\lambda)}\right]}{L} \quad (3)$$

where

$P_{out}(\lambda)$  is the output power,  $P_{in}(\lambda)$  is the input power,  $A(\lambda)$  is the attenuation,  $\alpha(\lambda)$  is the attenuation coefficient, L is the fiber length,  $T_{ref}(\lambda)$  is the reference value of transmission at room temperature ( $25^{\circ}\text{C}$ ), and  $T_{out}(\lambda)$  is the transmission at different temperatures on test.

## 3. Results and discussion

### 3.1. Temperature effects on the fiber transmission loss coefficient

The sample was tested gradually by heating up and cooling down. Fig. 2 shows the transmission loss on  $850\text{ nm}$  wavelength at range ( $-100^{\circ}\text{C} \sim 100^{\circ}\text{C}$ ) of temperature. For the line increasing 1, the temperature was increased from  $30^{\circ}\text{C}$  to  $100^{\circ}\text{C}$  and obtained that the high attenuation coefficient was  $4.27\text{ dB}/\text{km}$  at  $80^{\circ}\text{C}$  and the low attenuation coefficient for this increasing was  $2.73\text{ dB}/\text{km}$  at  $95^{\circ}\text{C}$ .

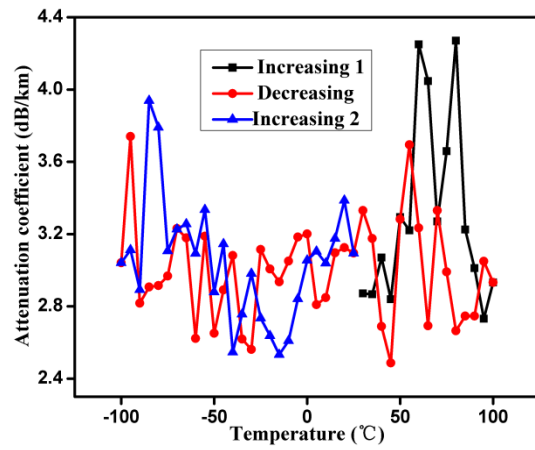


Fig. 2. Transmission loss coefficient at 850 nm wavelength

From  $100^{\circ}\text{C}$  the temperatures was decreased to  $-100^{\circ}\text{C}$  the attenuation coefficient was  $2.49, 3.74\text{ dB}/\text{km}$  at  $45, -95^{\circ}\text{C}$  respectively. Finally, we cool the temperature to room temperature  $25^{\circ}\text{C}$  and found the attenuation coefficient was  $2.53, 3.93\text{ dB}/\text{km}$  at  $-15, -85^{\circ}\text{C}$  respectively. Compared with all temperature conditions, it was estimated that there was an optimum heat-treated temperature to decrease transmission loss, and the temperature can be near  $45^{\circ}\text{C}$ . Therefore, from  $-75^{\circ}\text{C} \sim 60^{\circ}\text{C}$  the attenuation coefficient was fluctuating at range  $2.487\text{ dB}/\text{km} \sim 3.386\text{ dB}/\text{km}$ . And at the ends of the both sides of high and Low-temperature the attenuation coefficient was relatively large, and it's depending on the glass temperature point, but in the range  $-75^{\circ}\text{C} \sim 60^{\circ}\text{C}$  the attenuation coefficient was relatively small fluctuations. The attenuation loss spectra of the sample in the range  $-75^{\circ}\text{C} \sim 60^{\circ}\text{C}$  of cooling process and heating process at the same temperature has low differences, which confirmed that the fabricated optical fiber has good temperature resistance and high-temperature sensitivity. The high transmission loss coefficient was observed at  $80^{\circ}\text{C}$ , and the low transmission loss coefficient observed at  $45^{\circ}\text{C}$ .

The transmission loss coefficient with changes in temperature is a non-linear relationship, it is worth noting that it is the square relationship with variables by proportional, and this is just a random fluctuation. As a result, the sharp peak at  $80^{\circ}\text{C}$  could be observed in the

first shoot up. Fig. 3 shows the transmission loss coefficient of 1050 nm wavelength. There was a significant difference when comparing with 850 wavelengths. It was found that the attenuation was very high at the end of low-temperature (5.5 dB/km at  $-100^{\circ}\text{C}$ ) and low at the end of high temperature for decreasing temperature (0.9 dB/km at  $50^{\circ}\text{C}$ ). This indicates that this kind of optical fiber fits to 850nm. The maximum temperature measured is  $100^{\circ}\text{C}$  which is not sufficient for many applications.

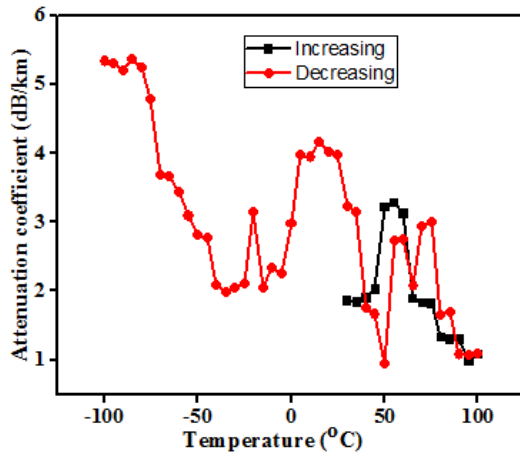


Fig. 3. Transmission loss coefficient of 1050 nm wavelength

### 3.2. Analysis on transmission loss changes at both high and low temperature side

Fig. 4 compares the EPR spectra before and after high low-temperature cycle. EPR due to the paramagnetic

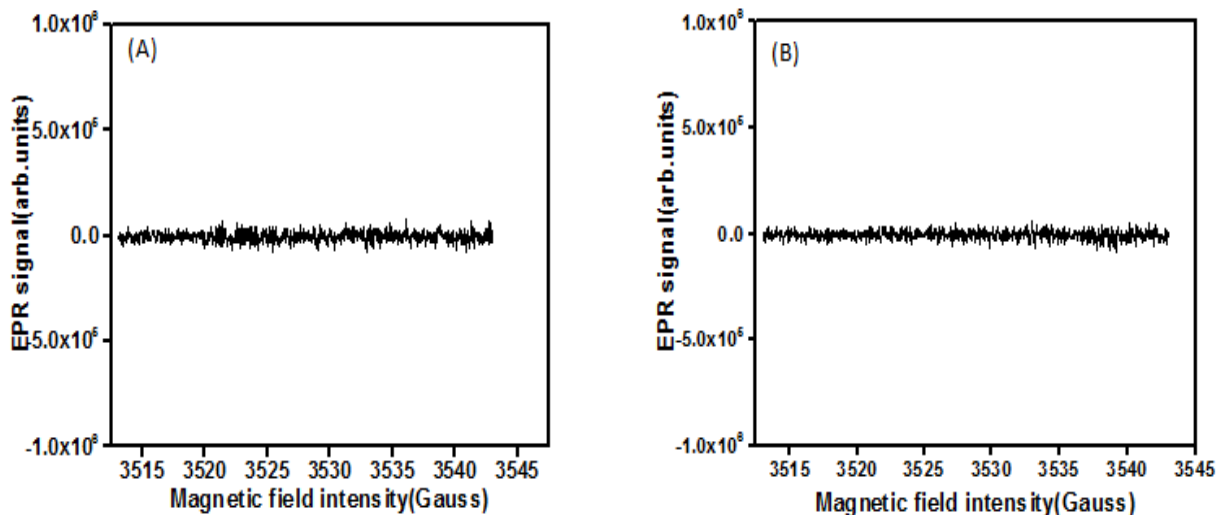


Fig. 4. Different EPR spectra of large-core optical fiber high-low temperature cycle (A) before high-low temperature cycle; (B) after high-low temperature cycle

The change from conduction mode to radiation mode into the cladding causes micro-bending loss, and produce

defects in optical fiber non-bridging oxygen hole center (NBOHC),  $Si - E'$  and oxygen hole center (OHC).

There is no resonance peak reveal in the signal of the sample before or after high low-temperature cycle. This indicates that EPR has no defects in the  $SiO_2$ . From the form of resonance signal the  $E'$  can be found in  $SiO_2$ [17]. Also, first differential spectral analysis can be obtained through a large core optical fiber, which does not show significant energy paramagnetic resonance signal after temperature cycling. It was shown that in the high and low-temperature range ( $-100^{\circ}\text{C} \sim 100^{\circ}\text{C}$ ), the core and cladding parts have a little or no presence of paramagnetic defects. Therefore, in large-core energy optical fiber suggests that the chemical bond in that range of temperature not occurred. It was also revealed the paramagnetic defects in large-core optical fiber during the preparation of the energy produced little or no presence of defects.

Since the optical fiber radius is much larger than 15cm much larger than the G.651.1 multimode fiber 15mm, so the bending loss can disregard. However, the coating by acrylic resin leads to thermal expansion and shrinkage of the optical fiber extension at high and low temperature. For shrinkage elongation at high-low temperature, the linear expansion coefficient is about  $10^{-3} \sim 10^{-4} \text{m}/^{\circ}\text{C}$ , and the expansion coefficient of the large core optical fiber is approximately  $10^{-7} \text{m}/^{\circ}\text{C}$ . The effect of temperature expansion of the two different depends on high temperatures, coated optical fiber length, fiber stress; low temperatures, short coated optical fiber and fiber stress. When the stress reaches a certain level, the optical signal transmission in optical fiber should be changed.

additional transmission loss on fiber. As result of the temperature changing, the fiber coating and the expansion

effects of high temperature, the coating layer is bare fiber elongation, so that the optical fiber was generated transverse and longitudinal tensile stress; when the temperature is low, the coating layer is bare fiber shortening by transverse and longitudinal contraction and the optical fiber compressive stress. When temperature increases, the micro-bending loss modification would reduce with an increment of thickness of coating layer and will rise. The rise of the thickness of coating layer makes the micro-bending loss. The temperature increase affecting the fiber do the micro-bending loss reduction. And also the micro-bending loss expects the tensile pressure applied on the optical fiber [18].

For large core energy optical fiber, the transmission loss coefficient at high and low temperature at range ( $-75^{\circ}\text{C} \sim 60^{\circ}\text{C}$ ) was due fluctuation. The glass transition temperature of optical fiber coating was analyzed by differential scanning calorimetry, where the heating rate is set to  $10\text{K}/\text{min}$ , the initial temperature is set to  $25^{\circ}\text{C}$ . The results of the glass transition are shown in Fig. 5 and show that the starting point is  $39.1^{\circ}\text{C}$ , the midpoint is  $65.1^{\circ}\text{C}$ , and the termination point is  $91^{\circ}\text{C}$ . However, the glass transition temperature of the coating layer is  $65.1^{\circ}\text{C}$ . When the temperature is higher than the glass transition temperature of the polymer, the polymer deformation will change significantly. In a heating process, the coating stress has released the layer and core. At the end of high and low temperature, material deformation was reflected with small transmission loss coefficient, but the transmission loss coefficient and the temperature were relatively small. When the temperature is decreased at the end of the high and low glass transition temperature, the coating layer is transformed from viscoelastic state to glass state and its deformation is reduced. At the same time, at low temperature, small shrinkage and small stress, the transmission loss coefficient of the fiber would have fewer effects. It was explained that the transmission loss coefficient at temperature  $-75^{\circ}\text{C} \sim 60^{\circ}\text{C}$  has small fluctuation phenomenon.

The experiment showed that the temperature was not reached to the melting point of the coating layer ( $106^{\circ}\text{C}$ ). Therefore, the large core energy fiber after high low-temperature cycle returned to the room temperature and produced a certain amount of permanent deformation. Compared with the high low-temperature cycle test before coating; the fiber has produced a certain amount of stress and elongation.

### 3.3. Analysis on attenuation coefficient relaxation after thermal treatment

At the further study on the thermal cycle experiment, the transmission loss coefficient for the first window ( $850\text{nm}$ ) was obtained at room temperature ( $25^{\circ}\text{C}$ ) for 50 days. Fig. 6 shows that the transmission loss coefficient decreased from  $3.095\text{dB}/\text{km}$  to  $2.353\text{dB}/\text{km}$  with increasing time. In the first 5 days, the transmission loss coefficient was decreased greatly because after annealing at room temperature and after high low-temperature cycle generated in the experiment the stress

was released. At the same time, the optical transmission loss coefficient was lower than the initial transmission loss coefficient; because the coated fiber in the preparation process has a certain stress. After the high and low-temperature cycling, the residual stress in the optical fiber is further released after the annealing at room temperature, so the transmission loss coefficient of the fiber was lower than that of the beginning experiment. Therefore, the stress reduced by the heating-cooling process, because the increase of coating layer thickness would raise the radial stress component; the stress component in the coating layer does not depend on the layer thickness but is reduced by raising the temperature and is dependent on the thermal expansion.

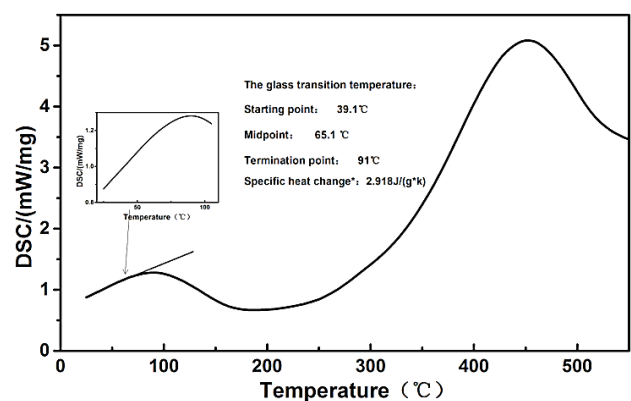


Fig. 5. Glass transition curves of the large core optical fiber

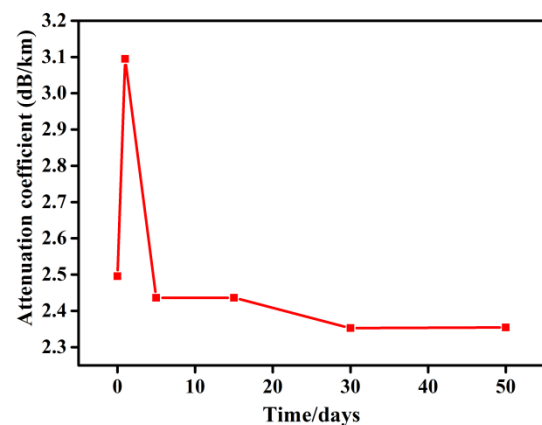


Fig. 6. Optical transmission loss coefficients at room temperature for 50 days ( $850\text{nm}$  wavelength)

## 4. Conclusions

In summary, the effect of temperature on the transmission loss of large-core optical fiber was studied. The transmission loss coefficient with varying of temperatures was a non-linear. It was also estimated that there was an optimum heat-treated temperature to decrease transmission loss, and the temperature can be near  $45^{\circ}\text{C}$ . This kind of optical fiber with F- doped on optical fiber has good temperature resistance and high-temperature

sensitivity, it is better to use in a harsh environment and a promising temperature sensor. Through establishing stress model, the transmission loss coefficient demonstrated to have greater fluctuation at the end of high low-temperature and has less fluctuation at a range  $-75^{\circ}\text{C} \sim 60^{\circ}\text{C}$ . For core and cladding parts, paramagnetic defects were found; the result indicates that the large core energy fiber preparation in the rarity of paramagnetic defects does not exist. For several days, the optical transmission loss coefficient was lower than the preliminary transmission loss coefficient.

### Acknowledgments

This work has been partly supported by 863 project (2013AA031502) and Science and Technology Support Project (20158BAI01B05).

### References

- [1] W. F. Yeung, A. R. Johnston, *Applied Optics* **17**(23), 3703 (1978).
- [2] E. Li, X. Wang, C. Zhang, *Applied Physics Letters* **89**(9), 091119 (2006).
- [3] J. Ju, et al., *IEEE Photonics Technology Letters* **18**(20), 2168 (2006).
- [4] D. S. Moon, et al., *Optics Express* **15**(13), 7962 (2007).
- [5] F. Pang, et al., *Optics Express* **16**(17), 12967 (2008).
- [6] X. Fu, et al., *Optics Express* **23**(3), 2320 (2015).
- [7] R. Dils, *Journal of Applied Physics* **54**(3), 1198 (1983).
- [8] A. Mehta, W. Mohammed, E. G. Johnson, *IEEE Photonics Technology Letters* **15**(8), 1129 (2003).
- [9] J. Zhang, S. Peng, *Photonics and Optoelectronic (SOPO)*, 2010 Symposium on, 2010.
- [10] A. Kumar, R. K. Varshney, P. Sharma, *Optics Communications* **219**(1), 215 (2003).
- [11] F. Favero, et al., *Optics Express* **21**(25), 30266 (2013).
- [12] J. Demas, et al., *Optics Letters* **37**(18), 3768 (2012).
- [13] A. Van Newkirk, et al., *Optics Letters* **39**(16), 4812 (2014).
- [14] J. E. Antonio-Lopez, et al., *Optics Letters* **39**(15), 4309 (2014).
- [15] A. Honda, et al., *Journal of Nuclear Materials* **367–370**, Part B, 1117 (2007).
- [16] Z. V. Vardeny, *Nature* **416**(6880), 489 (2002).
- [17] J. Wen, et al., *Journal of Applied Physics* **107**(4), 044904 (2010).
- [18] F. E. Seraji, G. Toutian, *Progress in Quantum Electronics* **30**(6), 317 (2006).

---

\*Corresponding author: jinzhong\_wang@hit.edu.cn